

Oxygen Isotope Effects on Electron Transfer to O₂ Probed Using Chemically Modified Flavins Bound to Glucose Oxidase

Justine P. Roth,^{*,‡} Roseanne Wincek,[†] Gabrielle Nodet,[†] Dale E. Edmondson,[§] William S. McIntire,^{||,⊥} and Judith P. Klinman^{*,†}

Contribution from the Departments of Chemistry and of Molecular and Cell Biology, University of California, Berkeley, California 94720, and the Department of Chemistry, The Johns Hopkins University, 3400 North Charles Street, Baltimore, Maryland 21218

Received May 19, 2004; E-mail: jproth@jhu.edu; klinman@socrates.berkeley.edu

Abstract: Apo-glucose oxidase has been reconstituted with flavins modified in the 7 and 8 positions and characterized with regard to the catalytic rate of O₂ reduction and oxygen-18 isotope effects on this process. Kinetic studies as a function of driving force indicate a reorganization energy for electron transfer to O₂ of $\lambda = 28$ kcal mol⁻¹ at optimal pH, which is similar to the value obtained earlier from temperature dependencies of rates (Roth, J. P.; Klinman, J. P. *Proc. Natl. Acad. Sci. U.S.A.* **2003**, *100*, 62–67). For the various enzyme-bound flavins, competitive oxygen-18 kinetic isotope effects fall within the narrow range of 1.0266(5) to 1.0279(6), apparently because of the dominant contribution of outer-sphere reorganization to the activation barrier; within the context of semiclassical and quantum mechanical electron transfer theories, the magnitude of the isotope effects reveals the importance of nuclear tunneling.

Introduction

Establishing a set of basic principles that can be used to predict the reactivity of O₂ has far-reaching consequences, possibly leading to improved biosensors¹ and fuel cells² and to the development of “green” catalysts for use in selective oxidation reactions.³ The inhibition of O₂ reduction has further implications in biological systems where reactive oxygen species (ROS) are known to cause damage of lipids,⁴ proteins,⁵ and DNA.^{5a,6} While it is understood that reduction of O₂ in solution by organic and inorganic reactants occurs predominantly by

electron transfer,⁷ enzymes may catalyze these processes using highly evolved strategies which, at present, are subject to debate.^{8,9}

Glucose oxidase is an ideal model system for examining the catalyzed reduction of O₂. This flavoprotein oxidase is representative of a class of enzymes that couples substrate dehydrogenation to the production of H₂O₂. A wealth of structural information, from X-ray diffraction¹⁰ and NMR,¹¹ is available on the protein from *Aspergillus*.¹² Active glucose oxidase is a homodimer with each subunit containing 1 equiv of non-covalently bound flavin adenine dinucleotide (FAD) ~15 Å below the protein surface. The enzyme is quite robust, maintain-

[†] University of California, Berkeley.

[‡] The Johns Hopkins University.

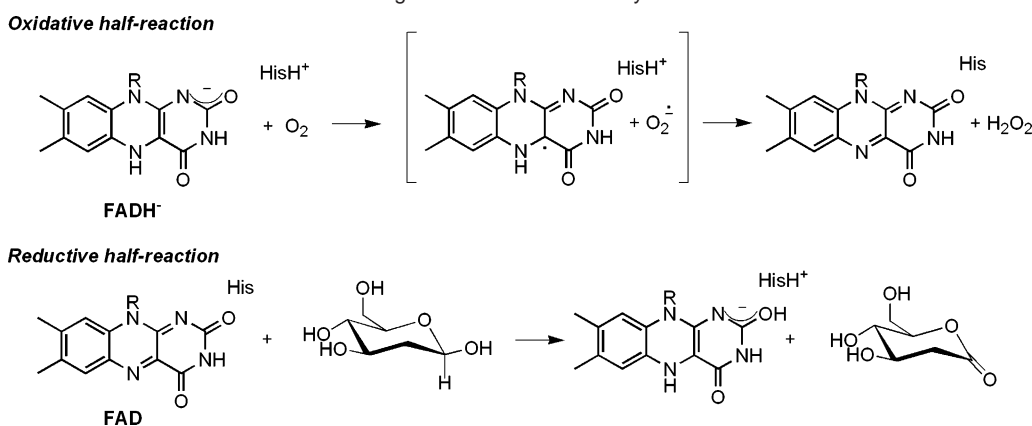
[§] Departments of Biochemistry and Chemistry, Emory University School of Medicine, Atlanta, GA 30322.

^{||} Division of Molecular Biology, Veterans Affairs Medical Center, San Francisco, CA 94121.

[⊥] Department of Biochemistry and Biophysics, University of California, San Francisco, CA 94121.

- (1) (a) Riklin, A.; Katz, E.; Willner, I.; Stocker, A.; Bueckmann, A. F. *Nature (London)* **1995**, *376*, 672–675. (b) Alvarez-Icaza, M.; Kalisz, H. M.; Hecht, H. J.; Aumann, K. D.; Schomburg, D.; Schmid, R. D. *Biosens. Bioelectron.* **1995**, *10*, 735–742. (c) Trojanowicz, M.; Geschke, O.; Krawczynski vel Krawczyk, T.; Cammann, K. *Sens. Actuators, B* **1995**, *B28*, 191–199.
- (2) (a) Chen, T.; Barton, S. C.; Binyamin, G.; Gao, Z.; Zhang, Y.; Kim, H.-H.; Heller, A. *J. Am. Chem. Soc.* **2001**, *123*, 8630–8631. (b) Sasaki, S.; Karube, I. *Trends Biotechnol.* **1999**, *17*, 50–52.
- (3) (a) Anastas, P. T.; Warner, J. C. *Green Chemistry Theory and Practice*; Oxford University Press: New York, 1998. (b) Boettcher, A.; Birnbaum, E. R.; Day, M. W.; Gray, H. B.; Grinstaff, M. W.; Labinger, J. A. *J. Mol. Catal. A: Chem.* **1997**, *117* (*Proceedings of the 6th International Symposium on the Activation of Dioxygen and Homogeneous Catalytic Oxidation, 1996*), 229–242. (c) Valderrama, B.; Marcela, A.; Vazquez-Duhalt, R. *Chem. Biol.* **2002**, *9*, 555–565. (d) Weinstock, I. A.; Barbuzzl, E. M. G.; Wemple, M. W.; Cowan, J. J.; Reiner, R. S.; Sonnen, D. M.; Heintz, R. A.; Bond, J. S.; Hill, C. L. *Nature (London)* **2001**, *414*, 191–195.
- (4) (a) Pratt, D. A.; Mills, J. H.; Porter, N. A. *J. Am. Chem. Soc.* **2003**, *125*, 5801–5810. (b) Fessel, J. P.; Porter, N. A.; Moore, K. P.; Sheller, J. R.; Roberts, L. J., II. *Proc. Natl. Acad. Sci. U.S.A.* **2002**, *99*, 16713–16718. (c) Leonarduzzi, G.; Arkan, M. C.; Basaga, H.; Chiarpotto, E.; Sevanian, A.; Poli, G. *Free Radical Biol. Med.* **2000**, *28*, 1370–1378.

- (5) (a) Marnett, L. J.; Riggins, J. N.; West, J. D. *J. Clin. Invest.* **2003**, *111*, 583–593. (b) Dean, R. T.; Fu, S.; Stocker, R.; Davies, M. *J. Biochem. J.* **1997**, *324*, 1–18. (c) Ghezzi, P.; Bonetto, V. *Proteomics* **2003**, *3*, 1145–1153.
- (6) (a) Tallman, K. A.; Tronche, C.; Yoo, D. J.; Greenberg, M. M. *J. Am. Chem. Soc.* **1998**, *120*, 4903–4909. (b) Breen A. P.; Murphy J. A. *Free Radical Biol. Med.* **1995**, *18*, 1033–1077.
- (7) (a) Lind, J.; Shen, X.; Merényi, Jonsson, B. Ö. *J. Am. Chem. Soc.* **1989**, *111*, 7654–7655. (b) Eberson, L.; González-Luque, R.; Lorentzon, J.; Merchán, Roos, B. O. *J. Am. Chem. Soc.* **1993**, *115*, 2898–2902. (c) Eberlein, G.; Bruice, T. C. *J. Am. Chem. Soc.* **1983**, *105*, 6685–6697. (d) Kemal, C.; Chan, T. W.; Bruice, T. C. *J. Am. Chem. Soc.* **1977**, *99*, 7272–7286. (e) Eberlein, G.; Bruice, T. C.; Lazarus, R. A.; Henrie, R.; Benkovic, S. J. *J. Am. Chem. Soc.* **1984**, *106*, 7916–7924. (f) Zahir, K.; Espenson, J. H.; Bakac, A. *J. Am. Chem. Soc.* **1988**, *110*, 5059–5063. (g) McDowell, M. S.; Espenson, J. H.; Bakac, A. *Inorg. Chem.* **1984**, *23*, 2232–2236. (h) Stanbury, D. M.; Haas, O.; Taube, H. *Inorg. Chem.* **1980**, *19*, 518–524.
- (8) (a) Klinman, J. P. *J. Biol. Inorg. Chem.* **2001**, *6*, 1–13. (b) Massey, V. *J. Biol. Chem.* **1994**, *269*, 22459–22462. (c) Babcock, G. T. *Proc. Natl. Acad. Sci. U.S.A.* **1999**, *96*, 12971–12973.
- (9) *Active Oxygen in Biochemistry*; Valentine, J. S., Foote, C. S., Greenberg, A., Liebman, J. F., Eds.; Chapman and Hall: New York, 1995.
- (10) Wohlfahrt, G.; Witt, S.; Hendle, J.; Schomburg, D.; Kalisz, H. M.; Hecht, H.-J. *Acta Crystallogr., Sect. D* **1999**, *55*, 969–977.
- (11) Sanner, C.; Macheroux, P.; Rüterjans, H.; Müller, F.; Bacher, A. *Eur. J. Biochem.* **1991**, *196*, 663–672.
- (12) Frederick, K. R.; Tung, J.; Emerick, R. S.; Masiarz, F. R.; Chamberlain, S. H.; Vasavada, A.; Rosenberg, S.; Chakraborty, S.; Schopfer, L. M.; Massey, V. *J. Biol. Chem.* **1990**, *265*, 3793–3802.

Scheme 1. Oxidative and Reductive Half-Reactions during Glucose Oxidase Catalysis

ing high rates of turnover over wide ranges of pH and temperature. Most importantly, large quantities of the apo-protein lacking FAD can be isolated and reconstituted with unnatural flavins in high yields.

A ping-pong kinetic mechanism has been established for glucose oxidase wherein the reaction of the sugar and release of the lactone product occur prior to O₂ entering the catalytic cycle.¹³ This simple behavior allows the catalytic cycle to be defined in terms of an oxidative half-reaction, where FADH⁻ is oxidized by O₂, and a reductive half-reaction, where FAD is reduced by an equivalent of bound sugar (Scheme 1).

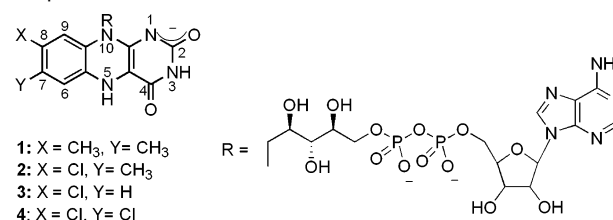
A single histidine residue in the proximity to FADH⁻ has been implicated as a Lewis acid catalyst during the oxidative half-reaction.¹⁴ Based on the observation of large oxygen-18 kinetic isotope effects on the second-order reaction with O₂ (¹⁸k_{cat}/K_M ~ 1.028), pH-independent limiting rate constants, and the absence of solvent kinetic isotope effects, electron transfer has been proposed to occur in the first irreversible step. Mutagenesis studies have suggested that HisH⁺516 is a key residue in maintaining the dipolar network of the active site, which is apparently preorganized such that electron transfer requires very little change in protein structure and solvation.

In the present study, the dependence of O₂ reduction rates on reaction free energy is examined to explore further electron transfer in glucose oxidase. The results compare favorably with previous studies of rates as a function of temperature; the aggregate data support an electron-transfer mechanism and activation-barrier lowering due to reduction of reorganization energy within the protein. Analysis of the reorganization energy together with the oxygen-18 kinetic isotope effects is used to address the nature of the reaction coordinate for the catalyzed electron-transfer reduction of O₂.

Results

Driving-force studies were performed using the enzyme-bound cofactors shown in Scheme 2. Spectroscopic characterizations of the various flavins bound to glucose oxidase have been previously reported.¹⁵ Herein we examine the kinetics of reactions of these modified enzymes for the first time.

Preparation of Enzymes. Apo-glucose oxidase was prepared by partial unfolding of the protein under strongly acidic

Scheme 2. Native Flavin (1) and Flavin Analogues (2–4) Incorporated into Glucose Oxidase

conditions followed by removal of the FAD by size-exclusion chromatography. Care was taken to exclude light and keep the enzyme at 0 °C during the unfolding process. A single chromatographic separation was sufficient to isolate apo-protein with less than 0.3% residual glucose oxidase activity. Yields were typically greater than 50%. The apo-protein stored at -80 °C for several months could be quantitatively reconstituted with native and chemically modified flavins, and full enzymatic activity recovered.

The FAD analogues were prepared from chemically modified riboflavin precursors¹⁶ using excess ATP and FAD synthetase.¹⁷ Similarly high affinities of glucose oxidase for all flavins were indicated although quantitative binding studies were not undertaken. Addition of stoichiometric amounts of flavin to the apo-protein gave high yields of holoprotein within hours at 0 °C. Addition of stoichiometric glucose to anaerobic solutions of the holoprotein resulted in bleaching of the optical absorbance at ca. 450 nm indicating reduction of the bound flavin. The enzyme-bound flavin could also be reduced under initially aerobic conditions in the presence of excess substrate because of the fast enzyme turnover and depletion of O₂ from solution. The quantitative reduction of flavin supports the view that all of the cofactor present was bound to the enzyme in a catalytically productive conformation. The optical absorbance changes observed during titrations of the enzyme-bound modified flavins were similar to those observed with the native enzyme from which FAD had never been removed.¹² Control experiments

(13) (a) Gibson, Q. H.; Swoboda, B. E. P.; Massey, V. *J. Biol. Chem.* **1964**, *239*, 3927–3934. (b) Bright, H. J.; Gibson, Q. H. *J. Biol. Chem.* **1967**, *242*, 3927–3934.
 (14) Roth, J. P.; Klinman, J. P. *Proc. Natl. Acad. Sci. U.S.A.* **2003**, *100*, 62–67.

(15) (a) Massey, V.; Hemmerich, P. In *Flavins and Flavoproteins*; Massey, V., Williams, C. H., Eds.; Elsevier: Berlin, 1982. (b) Ghisla, S.; Massey, V. *Biochem. J.* **1986**, *239*, 1–12. (c) Massey, V.; Ghisla, S.; Moore, E. G. *J. Biol. Chem.* **1979**, *254*, 9640–9650. (d) Schopfer, L. M.; Massey, V.; Claiborne, A. *J. Biol. Chem.* **1981**, *256*, 7329–7337. (e) Fisher, J.; Spencer, R.; Walsh, C. *Biochemistry* **1976**, *15*, 1054–1064.
 (16) (a) Stankovich, M. T. In *Chemistry and Biochemistry of Flavoenzymes*; Müller, F., Ed. CRC Press: Boca Raton, FL, 1991. (b) Müller, F.; Massey, V. *J. Biol. Chem.* **1969**, *244*, 4007–4016.
 (17) Efimov, I.; Kuusk, V.; Zhang, X.; McIntire, W. S. *Biochemistry* **1998**, *37*, 9716–9723.

Table 1. Steady-State Kinetic Parameters for the Oxidation of Deoxyglucose (0.5 M) by O₂ at pH 5.0, 25 °C, and μ = 0.1 M (Uncertainties Reflect Two Standard Errors)

entry	enzyme	$k_{\text{cat}}/K_{\text{M}}(\text{O}_2)^a$ ($\times 10^{-6} \text{ M}^{-1} \text{ s}^{-1}$)	$K_{\text{M}}(\text{O}_2)^b$ (μM)
1	7,8-Me^c	1.6 ± 0.2^b	27 ± 8
2	8-Cl^{c,d}	0.39 ± 0.053	300 ± 48
3	7-H 8-Cl^d	0.31 ± 0.019	750 ± 200
4	7,8-Cl^{c,d}	0.075 ± 0.016	670 ± 400

^a From the linear portion of the Michaelis–Menten plot unless noted.

^b From nonlinear curve fitting to the Michaelis–Menten expression.

^c Prepared from 320 kDa recombinant protein.¹² ^d Prepared from 160 kDa commercial glucose oxidase.²³

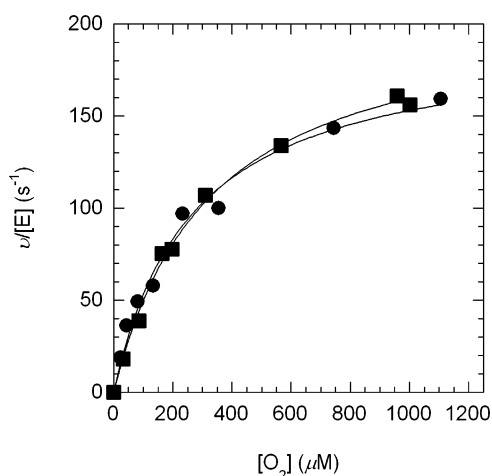


Figure 1. Observed rate constants ($v/[E]$) as a function of $[\text{O}_2]$ for **8-Cl GO** 160 kDa (squares) and 320 kDa (circles) proteins. Data are fitted to the Michaelis–Menten equation.

indicated that free FAD did not undergo reduction by excess glucose under the analogous conditions. No evidence was obtained that the free FAD exchanged or reacted with the enzyme-bound cofactor.

Electron-Transfer Kinetics. Steady-state experiments were performed using nanomolar concentrations of glucose oxidase and a working Clark electrode to determine micromolar changes in the concentration of dissolved O₂ as a function of time.¹⁸ To determine each rate constant, 8 to 10 measurements were performed at varying concentrations of O₂ using 2-deoxyglucose as cosubstrate at concentrations from 6- to 10-fold above the enzyme saturation limit. Concentrations of O₂ were varied from 2×10^{-6} M to approximately 1.0×10^{-3} M by changing the partial pressures of O₂ and N₂ in gas mixtures used to saturate the reaction solutions at atmospheric pressure.

The rate constants, $k_{\text{cat}}/K_{\text{M}}(\text{O}_2)$, were estimated from the linear portions of the observed rate constant versus $[\text{O}_2]$ plots. The Michaelis constants, $K_{\text{M}}(\text{O}_2)$, were extracted from data at high and low concentration of O₂ fitted to the Michaelis–Menten expression. The results are presented in Table 1 with limits that reflect two standard errors. The kinetic parameters were determined to be reproducible among batches of reconstituted enzyme obtained from different sources of apo-protein and modified flavin. A typical plot is shown in Figure 1 for reaction of O₂ with **8-Cl GO**. As previously demonstrated for the native glucose oxidase, the second-order rate constants are indistinguishable for the different enzyme glycoforms.^{19,20}

(18) Hitchmann, M. L. *The Measurement of Dissolved Oxygen*; John Wiley: New York, 1978.

Native glucose oxidase (**7,8-Me GO**) contains the most electron-rich cofactor examined and reduces O₂ the fastest with $k_{\text{cat}}/K_{\text{M}}(\text{O}_2) = (1.6 \pm 0.2) \times 10^6 \text{ M}^{-1} \text{ s}^{-1}$. Following in order of decreased electron-releasing ability is **8-Cl GO**, $(3.9 \pm 0.5) \times 10^5 \text{ M}^{-1} \text{ s}^{-1}$; **7-H,8-Cl GO**, $(3.1 \pm 0.2) \times 10^5 \text{ M}^{-1} \text{ s}^{-1}$; and **7,8-Cl GO**, $(7.5 \pm 1.6) \times 10^4 \text{ M}^{-1} \text{ s}^{-1}$. Qualitatively the trend is consistent with electron transfer from flavin to O₂ in the first irreversible step of the oxidative half-reaction.

The kinetic parameter $K_{\text{M}}(\text{O}_2)$ is dramatically increased for enzymes containing modified flavins. Because of the limited solubility of O₂ under the experimental conditions, $K_{\text{M}}(\text{O}_2)$ greater than 5×10^{-4} M could not be accurately determined. As discussed previously, $K_{\text{M}}(\text{O}_2)$ is a complex kinetic parameter;¹⁴ its largest contribution comes not from the equilibrium binding of O₂, i.e., $K_{\text{d}}(\text{O}_2)$, but from rate constants associated with cofactor reduction.

Roughly the opposite trend is observed for the reductive half-reaction where the oxidized flavin accepts the equivalent of a hydride ion (H[−]) from the bound sugar. Experiments performed with [1-²H]-2-deoxyglucose, which contains a deuterium label at the anomeric carbon, ensured the highest degree of rate limitation by the bond cleavage step.²⁰ These experiments reveal rate constants that decrease with increased electron-releasing character of the cofactor. The **7,8-Cl GO** reacts fastest with $k_{\text{cat}}/K_{\text{M}}([1\text{-}^2\text{H}]\text{-2-deoxyglucose}) = (8.2 \pm 2.5) \times 10^2 \text{ M}^{-1} \text{ s}^{-1}$ followed by **8-Cl GO**, $(6.2 \pm 2.2) \times 10^2 \text{ M}^{-1} \text{ s}^{-1}$; **7-H,8-Cl GO**, $(4.6 \pm 2.2) \times 10^2 \text{ M}^{-1} \text{ s}^{-1}$; and **7,8-Me GO**, $(1.2 \pm 0.1) \times 10^2 \text{ M}^{-1} \text{ s}^{-1}$.

A full report on the reductive half-reaction is forthcoming.²¹ Here the data are provided to illustrate that the structural integrity of the active site and its sugar binding affinity are preserved in the enzymes containing modified cofactors. Assays containing high concentrations of O₂ (1.0×10^{-3} M) and 2-deoxyglucose at least 6-fold above K_{M} (5×10^{-1} M) revealed significantly higher turnover rates for **7,8-Cl GO**, **7-H,8-Cl GO**, and **8-Cl GO** than for **7,8-Me GO**. On these grounds, the modified enzymes containing electron-deficient flavins are superior catalysts for the oxidation of 2-deoxyglucose.

Thermodynamics of Electron Transfer. Reduction potentials have been measured for the native flavin bound to glucose oxidase at pH 5 and pH 9 using a spectro-electrochemical technique.²² We have subsequently reinterpreted these data¹⁴ in light of later results that indicated the fully reduced flavin exists predominantly as the anion FADH[−] at pH 5.0.¹¹ The one-electron reduction potentials corresponding to two prototropic forms of glucose oxidase are $E^{\circ'} = -0.065$ V at pH 5 and $E^{\circ'} = -0.12$ V at pH 12 versus NHE.¹⁴ The 0.055 V difference in the reduction potentials at high and low pH has been attributed to electrostatic stabilization of FADH[−] by HisH⁺516 which resides approximately 4 Å away from the N(1) position of the isoalloxazine ring.¹⁰ Consistent with this argument, HisH⁺516 lowers the pK_a of the flavin semiquinone from 8.3 in solution to 7.2 in glucose oxidase.²²

We have previously described a simplified continuum electrostatics model to address the stabilization energy of O₂[−] by

(19) Kohen, A.; Jonsson, T.; Klinman, J. P. *Biochemistry* **1997**, *36*, 2603–2611.

(20) Seymour, S. L.; Klinman, J. P. *Biochemistry* **2002**, *41*, 8747–8758.

(21) Roth, J. P.; Brinkley, D.; Wincek, R.; Edmondson, D. E.; McIntire, W. S.; Pershad, H.; Klinman, J. P., in preparation.

(22) Stankovich, M. T.; Schopfer, L. M.; Massey, V. *J. Biol. Chem.* **1978**, *253*, 4971–4979.

Table 2. Free Flavin Reduction Potentials at pH 7 and Thermodynamic Parameters for the Reduction of O₂ to O₂⁻ by Glucose Oxidase (Reduction Potentials Are Quoted versus NHE)

entry	flavin	$E^{\circ\prime}_{\text{meas}}^a$ (V)	$\Delta E^{\circ\prime}_{\text{meas}}^b$ (V)	$\Delta G^{\circ\prime}_{\text{meas}}$ (kcal mol ⁻¹) ^c	$E^{\circ\prime}_{\text{calc}}^{a,d}$ (V)	$\Delta E^{\circ}_{\text{calc}}^b$ (V)	$\Delta G^{\circ\prime}_{\text{calc}}^c$ (kcal mol ⁻¹)
1	7,8-Me	-0.208	0	-1.3	-0.225	0	-1.3
2	8-Cl	-0.152	0.056	0.023	-0.145	0.080	0.58
3	7-H 8-Cl	-0.144	0.064	0.21	-0.135	0.090	0.81
4	7,8-Cl	-0.126	0.082	0.62	-0.083	0.142	2.0

^a From ref 24. ^b The difference in $E^{\circ\prime}$ relative to the $E^{\circ\prime}$ for 1. ^c From eq 1 in text. ^d From Hammett analysis.

HisH⁺516.¹⁴ The 0.055 V shift in FADH⁻ reduction potentials at the high and low pH extremes, equivalent to $\Delta\Delta G^{\circ} = 1.3$ kcal mol⁻¹, is taken as a starting point. Assuming the dielectric properties of the environment surrounding the flavin and putative O₂⁻ product remain constant, the $\Delta\Delta G^{\circ}$ is adjusted by the effect of distance on the interaction energy of the two point charges. The ratio of closest approach distances to HisH⁺516, 4 Å for FADH⁻ and 1.5 Å for O₂⁻, is multiplied by $\Delta\Delta G^{\circ}$. The estimated electrostatic stabilization energy of O₂⁻, $\Delta\Delta G^{\circ} = 3.4$ kcal mol⁻¹, is equivalent to a +0.15V shift in the reduction potential of O₂. Comparable effects have been determined by cyclic voltammetry experiments on O₂ in polar aprotic solvents containing high concentrations of redox inactive metal cations.²³

The reduction potentials of the flavins used in this study are listed in Table 2. The $E^{\circ\prime}_{\text{meas}}$ were determined at pH 7 using potentiometric and spectrophotometric methods²⁴ and have been since confirmed by cyclic voltammetry studies as a function of pH.²⁵ As long as the sensitivity of $E^{\circ\prime}$ (FAD/FADH⁻) to changes in flavin substituent is similar to $\Delta E^{\circ\prime}$ (FADH[•]/FADH⁻), changes in the rate for one-electron O₂ reduction will correlate with the $\Delta E^{\circ\prime}$ values in Table 2 (cf. Figure 5). This will be the case when changes in flavin substituent lead to compensating effects on the ΔpK_a of FADH[•] and $\Delta E^{\circ\prime}$ (FAD/FAD^{•-}). We note that the trends in Table 2 have also been seen for $\Delta E^{\circ\prime}$ (FADH₂/FADH₂^{•+}) in acetonitrile, albeit with greater sensitivity to substituent.²⁶ The latter is likely due to the amplification of electronic effects on the formation of charged species in the lower dielectric solvent relative to reactions in water.

Edmondson and Ghisla²⁷ have compiled reduction potentials for flavin analogues at the riboflavin, flavin mononucleotide (FMN), and FAD levels and reported an excellent correlation of the electrochemical data with Hammett σ values.²⁸ Although the presence of the adenosine diphosphate moiety alters the reduction potential by 0.010–0.015 V,²⁹ this effect is small relative to the variation in potentials over the wide range of flavin analogues analyzed. The $E^{\circ\prime}_{\text{calc}}$ values predicted from the Hammett analysis²⁷ (Table 2) are used in this study under the premise that averaging data for twenty different derivatives minimizes the error associated with comparing cofactors at the riboflavin, FMN, and FAD levels.

Effective reaction driving forces ($\Delta G^{\circ\prime}$) for the one-electron reduction of O₂ by reduced flavins are provided in the final

columns of Table 2. Estimates were derived using an adapted version of the Nernst equation (eq 1) where F is Faraday's constant and n is the number of electron equivalents transferred in the reaction. The equation includes the standard state one-electron reduction potential for O₂ ($E^{\circ}_{\text{O}_2} = -0.16$ V versus NHE) corrected by 0.15 V for the electrostatic stabilization of O₂⁻ by HisH⁺516. Also included is the measured one-electron reduction potential for the native flavin *bound to glucose oxidase* at pH 5 ($E^{\circ\prime}_{7,8-\text{Me}} = -0.065$ V versus NHE)^{22,14} adjusted by $\Delta E^{\circ}_{\text{calc}} = (E^{\circ\prime}_{7-\text{X},8-\text{Y FAD}} - E^{\circ\prime}_{7,8-\text{Me FAD}})_{\text{calc}}$ derived from the measurements on the free flavins.

$$\Delta G^{\circ\prime} = -nF\{(E^{\circ}_{\text{O}_2} + 0.15 \text{ V}) - (-0.065 \text{ V} + \Delta E^{\circ}_{\text{calc}})\} \quad (1)$$

Oxygen-18 Kinetic Isotope Effects. Isotope effects on the second-order rate constant for reaction with O₂ ($^{18}k_{\text{cat}}/K_M$) were measured using natural abundance O₂. Beginning with concentrations close to the limit of dissolved O₂ at 30 °C and atmospheric pressure ($\sim 1 \times 10^{-3}$ M), samples of unreacted O₂ were isolated from reaction mixtures as a function of the percent O₂ consumed. All conditions were the same as those used to measure rates except for the presence of horseradish peroxidase and its substrate guaiacol which were used to scavenge the H₂O₂ produced. It has been shown that these reagents have no effect on $k_{\text{cat}}/K_M(\text{O}_2)$.¹⁴

Each oxygen isotope effect was determined from a minimum of six measurements, at least four of which were performed on independently prepared solutions. The reported $^{18}k_{\text{cat}}/K_M$ were derived from nonlinear fitting of data to eq 2, which describes the enrichment of ¹⁸O (R_o/R_f) in terms of the fraction of unreacted O₂ ($1 - f$). Samples were typically collected over the course of several hours at conversions that ranged from 10% to 80% of the O₂ initially present. Measurements on the time scale of minutes were performed using high concentrations of enzyme and found to be in excellent agreement with the long time scale measurements at the same percent conversion. The control experiments indicate that H₂O₂ is efficiently scavenged from reaction solutions over short and long time scales. On average, the fractional composition of ¹⁸O in unreacted O₂ varied by a factor of 2.5 from 0% to 80% conversion.

$$^{18}k_{\text{cat}}/K_M = \left[1 + \frac{\ln(R_f/R_o)}{\ln(1 - f)}\right]^{-1} \quad (2)$$

An ¹⁸O fractionation plot is shown in Figure 2 for the oxidation of 2-deoxyglucose by **7,8-Cl GO**. $^{18}k_{\text{cat}}/K_M = 1.0269$ (9) was derived from the 13 data points collected. A slightly smaller isotope effect with apparently less uncertainty, $^{18}k_{\text{cat}}/K_M = 1.0266(5)$, is obtained when the data are weighted by the

(23) (a) Sawyer, D. T.; Sobkowiak, A.; Roberts, J. L., Jr. *Electrochemistry for Chemists*; Wiley: New York, 1995. (b) Popisil, L.; Fuoco, R.; Papoff, P. *J. Electroanal. Chem.* **1988**, *256*, 83–93.

(24) Lowe, H. J.; Mansfield, C. *J. Biol. Chem.* **1956**, *221*, 983–992.

(25) Hasford, J. J.; Rizzo, C. *J. Am. Chem. Soc.* **1998**, *120*, 2251–2255.

(26) Eckstein, J. W.; Hastings, J. W.; Ghisla, S. *Biochemistry* **1993**, *32*, 404–411.

(27) Edmondson, D. E.; Ghisla, S. In *Flavins and Flavoproteins*; Ghisla, S., Kroneck, P., Macheroux, P., Sund, H., Eds.; Rudolf Weber: Berlin, 1999.

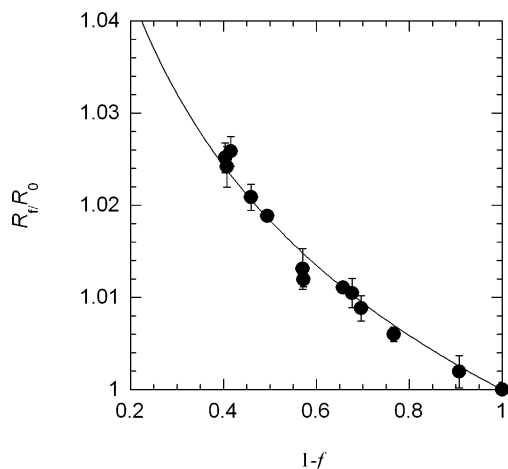
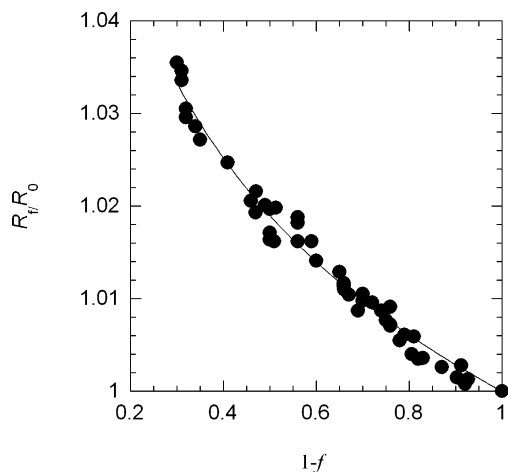
(28) Hansch, C.; Leo, A.; Taft, R. W. *Chem. Rev.* **1991**, *91*, 165–195.

(29) Draper, R. D.; Ingraham, L. L. *Arch. Biochem. Biophys.* **1968**, *125*, 802–808.

Table 3. Competitive Oxygen-18 Kinetic Isotope Effects with Uncertainties Reflecting Two Standard Errors

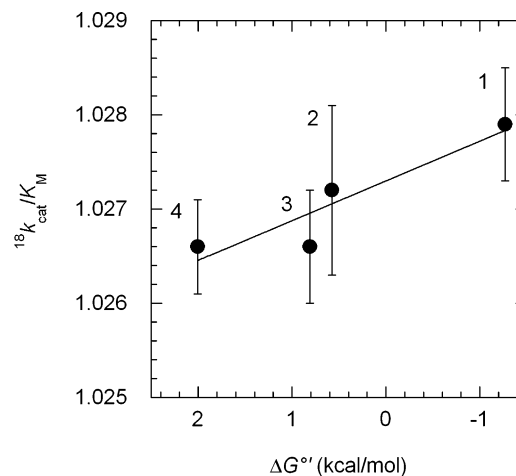
entry	enzyme	$^{18}k_{\text{cat}}/K_{\text{M}}(\text{O}_2)^{a,b}$	R^c	$^{18}k_{\text{cat}}/K_{\text{M}}(\text{O}_2)^{a,d}$	R^e	total pts
1	7,8-Me	$1.0279 \pm 0.0006^{d,f}$	0.990	$1.0279 \pm 0.0006^{b,d}$	0.990	49 (23) ^e
2	8-Cl	1.0256 ± 0.0020	0.976	1.0274 ± 0.0009	0.970	9 (7)
3	7-H 8-Cl	1.0264 ± 0.0016	0.992	1.0266 ± 0.0006	0.997	6 (4)
4	7,8-Cl	1.0269 ± 0.0009	0.994	1.0266 ± 0.0005	0.992	13 (9)

^a Measured at pH 5.0 and 298 K in the presence of 2-deoxyglucose ($(3-6) \times 10^{-2}$ M). ^b From unweighted data fitted to eq 2 unless noted. ^c The correlation coefficient determined using the general curve fit function in Kaleidagraph. ^d From weighted data fitted to eq 2. ^e Data collected by three researchers over a five-year period. ^f At pH 5.0 and 9.0 as described in ref 14.

**Figure 2.** ^{18}O fractionation (R_f/R_0) versus percent O_2 unconsumed ($1-f$) for the reaction of **7,8-Cl GO** with O_2 . Data are fitted to eq 2 and weighted by the experimentally determined variability.**Figure 3.** ^{18}O fractionation (R_f/R_0) versus percent O_2 unconsumed ($1-f$) for the reaction of **7,8-Me GO** with O_2 . Data are fitted to eq 2.

precision in R_f/R_0 . Precision was assessed by repeated measurements of the fractional composition of ^{18}O in natural abundance O_2 at 0% conversion. Ten independent measurements indicated that the variability was between 2.7% and 3.9% of the total ^{18}O content for different samples collected on different days over the course of six months. The errors estimated in this way are comparable to the error determined for the largest unweighted data set shown in Figure 3 for **7,8-Me GO**, which includes measurements by three different researchers over a five-year period.

Isotope Effects at Varying Driving Force. One goal of the present studies was to investigate possible variations in the oxygen-18 kinetic isotope effect as a function of the driving force for electron transfer to O_2 . Glucose oxidase was selected

**Figure 4.** $^{18}k_{\text{cat}}/K_{\text{M}}$ as a function of $\Delta G^{\circ'}$ calc from entries 1–4 in Tables 2 and 3.

for these studies on the basis of its uncomplicated kinetic behavior and well-defined electron-transfer mechanism.

The $^{18}k_{\text{cat}}/K_{\text{M}}$ for glucose oxidase containing native and modified flavin cofactors are presented in Table 3 and Figure 4. The error-weighted results indicate that $^{18}k_{\text{cat}}/K_{\text{M}}$ ranges from 1.0279 to 1.0266 for $\Delta G^{\circ'}$ values between -1.3 and 2.0 kcal mol $^{-1}$. Over this range of driving forces, the observed rate constants decrease nearly 20-fold. The largest difference in $^{18}k_{\text{cat}}/K_{\text{M}}$ is observed for the most electron-deficient **7,8-Cl GO** and the most electron-rich **7,8-Me GO** enzymes, although the size of the errors precludes a rigorous analysis of any trend.

The qualitative correlations between rates and driving force and the near invariance of the oxygen-18 kinetic isotope effects (Tables 1–3) are consistent with electron transfer occurring in the first kinetically irreversible step of the reaction where O_2 is reduced to H_2O_2 . A departure from this mechanism is entertained below because subsequent steps may contribute to the observed $k_{\text{cat}}/K_{\text{M}}(\text{O}_2)$, resulting in the kinetic complexity encountered in many enzymatic processes.³⁰ For example, if rates were reflected in part by a reaction involving combination of flavin semiquinone and O_2^- , acceleration with increasing electrochemical potential of the flavin would be expected. A hydrogen atom abstraction from the flavin semiquinone by O_2^- in a subsequent step should show a similar trend between the rate and driving force as electron transfer; however this mechanism is inconsistent with the absence of solvent isotope effects on $k_{\text{cat}}/K_{\text{M}}(\text{O}_2)$.¹⁴ Most importantly, extensive studies on the enzyme containing the native flavin have provided no evidence for the reversibility of the initial reaction with O_2 .^{13,14}

(30) Northrop, D. B. *J. Chem. Educ.* **1998**, *75*, 1153–1157.

Discussion

Theoretical Basis for Electron-Transfer Rates. The classical Marcus theory formalism expresses the free energy barrier to an electron transfer in terms of the intersection point of two harmonic oscillators with equal curvature. It follows that ΔG^\ddagger is a function of the effective Gibbs free energy of reaction ($\Delta G^{\circ\prime}$) and the intrinsic reorganization energy (λ) according to eq 3.^{31,32}

$$\Delta G^\ddagger = \frac{\lambda}{4} \left(1 + \frac{\Delta G^{\circ\prime}}{\lambda} \right)^2 \quad (3)$$

The λ is often defined classically as the sum of outer-sphere (λ_{out}) and inner-sphere (λ_{in}) terms which reflect contributions from orientation and polarization changes in the surrounding medium and intramolecular bond distortions, respectively.³³ Equation 4 gives the idealized response of the surroundings treated as a continuum of infinite dielectric to the electron transfer. Terms include a constant describing the vacuum permittivity of the charge transferred, $(\Delta e)^2 = 331.2 \text{ kcal mol}^{-1}$, optical and static dielectric constants (D_{op} and D_{s}), dielectric displacement vectors for the reactant and product states (D_1 and D_2), and a reaction cavity volume (V). Equation 5 expresses the free energy associated with changes in intramolecular bonding in terms of force constants and bond lengths. The f_i is the reduced normal mode force constant for the i th vibration, and Δ_i is the difference in the equilibrium nuclear positions of the reactant and product states.

$$\lambda_{\text{out}} = \frac{(\Delta e)^2}{8\pi} \left(\frac{1}{D_{\text{op}}} - \frac{1}{D_{\text{s}}} \right) \int (D_1 - D_2)^2 dV \quad (4)$$

$$\lambda_{\text{in}} = \frac{1}{2} \sum_i f_i \Delta_i^2 \quad (5)$$

The relationship between the energy barrier and the observed second-order rate constant for electron transfer is given by eq 6. The exponential term contains the thermally averaged free-energy activation barrier. The pre-exponential term contains an equilibrium constant describing the formation of a reactant complex (K_{R}) and frequency factors that describe the probability of reaction once the nuclear configuration of the activated complex is obtained.³² The κ_{el} is an electronic transmission coefficient defined according to the Landau and Zener equation, and ν_n describes the relaxation frequency of the solvent or an intramolecular mode that mediates passage of the system through the intersection region.³⁴

$$k_{\text{ET}} = K_{\text{R}} \kappa_{\text{el}} \nu_n \exp\left(\frac{-\Delta G^\ddagger}{RT}\right) \quad (6)$$

The electron-transfer reactions described by eq 6 can be electronically nonadiabatic or adiabatic. The former involve the population of electronically excited states and are characterized by $\kappa_{\text{el}} \ll 1$. When κ_{el} is very small, the pre-exponential in eq 6 is limited by the hopping frequency of the electron (ν_{el}), which

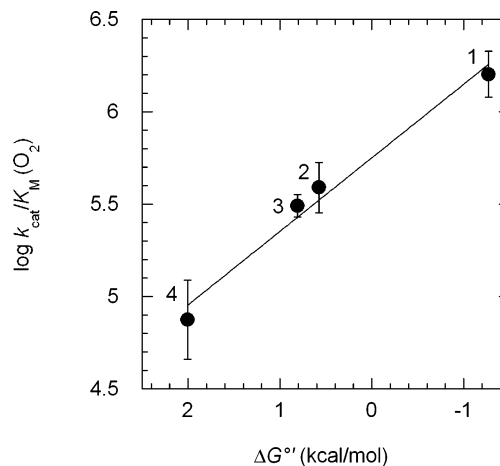


Figure 5. Free-energy relation for O₂ reduction by glucose oxidase containing modified flavin cofactors. Rate constants are from Table 1, and $\Delta G^{\circ\prime}_{\text{calc}}$ values are from Table 2.

depends on the electronic coupling of the reactant and product states. Over large distances, ν_{el} can limit the rate of reaction to an extent that is comparable to the free energy barrier.³⁴ For short-range reactions, κ_{el} is expected to be close to unity. This is the electronically adiabatic case where the reaction occurs exclusively along the ground-state energy surface and the pre-exponential part of eq 6 is dominated by ν_n . Since the nuclear response is typically on the time scale of picoseconds,³⁵ the free energy barrier largely determines the reaction rate. The electron transfer reaction in glucose oxidase is likely to be electronically adiabatic because the small molecular radius and freely diffusible nature of O₂ allow close approach to the FADH⁻. The adiabatic description is consistent with the large pre-exponential factors observed in studies of rates as a function of temperature.¹⁴

Application of Electron-Transfer Theory. The relationship between rates and reduction potentials is qualitatively consistent with a mechanism of rate-determining electron transfer from the fully reduced anionic flavin to O₂. In the present study λ is determined from the driving-force dependence of $k_{\text{cat}}/K_{\text{M}}(\text{O}_2)$. A linear correlation is obtained by plotting $\log k_{\text{cat}}/K_{\text{M}}(\text{O}_2)$ versus $\Delta G^{\circ\prime}$ (Figure 5). The linearity of the plot agrees with the predictions of classical Marcus theory for reactions in the normal driving-force regime.³⁶

To relate the results in Figure 5 to eq 3, the $k_{\text{cat}}/K_{\text{M}}(\text{O}_2)$ at $\Delta G^{\circ\prime} = 0$ is converted to a ΔG^\ddagger by assuming a pre-exponential factor of $10^{11} \text{ M}^{-1} \text{ s}^{-1}$ in eq 6.³² Use of this value implies that a fast and reversible formation of the reactant complex precedes the rate-limiting, adiabatic electron-transfer step. The $\log k_{\text{cat}}/K_{\text{M}}(\text{O}_2) = 5.8 \pm 0.2$ at $\Delta G^{\circ\prime} = 0$ gives ΔG^\ddagger (25 °C) = $7.1 \pm 0.2 \text{ kcal mol}^{-1}$ and $\lambda = 28 \pm 7 \text{ kcal mol}^{-1}$. To be as conservative as possible, the error in λ is reported as twice the correction factor of 0.15 V applied in eq 1. A somewhat poorer correlation is observed when $\Delta E^{\circ\prime}_{\text{meas}}$ values are used in place of $\Delta E^{\circ\prime}_{\text{calc}}$ in eq 1, presumably because the comparisons among the measured potentials for different flavin analogues are less reliable (see Results). However, the λ derived from $\Delta E^{\circ\prime}_{\text{meas}}$ is only 2 kcal mol⁻¹ greater than that derived from $\Delta E^{\circ\prime}_{\text{calc}}$.

(31) Marcus, R. A.; Sutin, N. *Biochim. Biophys. Acta* **1985**, *811*, 265–322.

(32) Sutin, N. *Prog. Inorg. Chem.* **1983**, *30*, 441–499.

(33) (a) Marcus, R. A. *J. Chem. Phys.* **1956**, *24*, 979–989. (b) Marcus, R. A. *J. Chem. Phys.* **1965**, *43*, 679–701.

(34) *Electron Transfer: From Isolated Molecules to Biomolecules Part One*; Jortner, J., Bixon, M., Eds.; Advances in Chemical Physics 106; Wiley: New York, 1999.

(35) Weaver, M. J. *Chem. Rev.* **1992**, *92*, 463–480.

(36) *Electron Transfer in Inorganic, Organic and Biological Systems*; Bolton, J. R., Mataga, N., McLendon, G., Eds.; Advances in Chemistry Series 228; American Chemical Society Press: Washington, DC, 1991.

The λ obtained from analysis of $\Delta E^{\circ'}_{\text{calc}}$ is in good agreement with that determined from temperature studies. Previously, rates of the oxidative half-reaction of **7,8 Me-GO** were studied over a 10 to 50 °C temperature range and analyzed in the adiabatic limit.^{14,37} At pH 5.0, plots of $\log k_{\text{cat}}/K_{\text{M}}(\text{O}_2)$ versus T^{-1} were found to be linear and rather flat, indicating $\Delta H^\ddagger = 2.3 \pm 0.8$ kcal mol⁻¹ and $\Delta S^\ddagger = -9 \pm 4$ cal mol⁻¹ K⁻¹. Since the original study, the activation parameters have been revised slightly to $\Delta H^\ddagger = 2.1 \pm 1.3$ kcal mol⁻¹ and $\Delta S^\ddagger = -11 \pm 4$ cal mol⁻¹ K⁻¹. The derived $\Delta G^\ddagger(25\text{ °C}) = 5.4 \pm 3.9$ kcal mol⁻¹ at $\Delta G^{\circ'} = -1.3$ kcal mol⁻¹ indicates $\lambda = 24 \pm 17$ kcal mol⁻¹. Thus, the driving-force studies confirm and allow a fairly significant refinement of the previous estimate of λ .

We have proposed that a single His affects the reduction of λ at low pH giving rise to catalytic rates of electron transfer from FADH⁻ to O₂.¹⁴ The recently determined activation parameters for the H516A mutant at pH 5.0 (see Supporting Information Figure S1) are consistent with this proposal. The $\Delta H^\ddagger = 10.0 \pm 0.6$ kcal mol⁻¹ and $\Delta S^\ddagger = 0 \pm 9$ cal mol⁻¹ K⁻¹ are in striking contrast to those of the wild-type enzyme at pH 5.0 but are similar to the activation parameters determined for the wild-type enzyme at pH 12.5, where $\Delta H^\ddagger = 8.6 \pm 1.3$ kcal mol⁻¹ and $\Delta S^\ddagger = -6 \pm 4$ cal mol⁻¹ K⁻¹.¹⁴ At high pH, $\Delta G^\ddagger(25\text{ °C}) = 10.4 \pm 2.2$ kcal mol⁻¹ and $\Delta G^{\circ'} = 0.92$ kcal mol⁻¹ indicate $\lambda = 40 \pm 8$ kcal mol⁻¹. Assuming $\Delta G^{\circ'}$ is the same for H516A at low pH and the wild-type enzyme at high pH, the $\Delta G^\ddagger(25\text{ °C}) = 10.0 \pm 3.0$ kcal mol⁻¹ corresponds to $\lambda = 40 \pm 12$ kcal mol⁻¹.

The linear correlation between rates and driving force indicates that the reactions of modified flavins with O₂ at low pH are characterized by the same λ . This also appears to be true in the reductive half-reaction of glucose oxidase where the flavin cofactors accept a hydride equivalent from bound sugar.²¹ Investigations of other flavoprotein oxidases containing modified cofactors have provided evidence that covalent flavin adducts are formed during catalysis.^{38,39} Specifically, studies of lactate oxidase⁴⁰ and *p*-hydroxybenzoate hydroxylase^{38a} have revealed break points in linear free-energy correlations that implicate complex equilibria preceding the redox steps in the catalytic cycle. No such behavior is seen for glucose oxidase where a linear relationship is observed over a range of driving force that is comparable to the height of the activation barrier. To our knowledge this is the first demonstration of cofactor substitution in a protein where the catalytic effects on both the oxidative and reductive half-reactions are in agreement with the predictions of classical Marcus theory.

Assumptions of the Adiabatic Model. The agreement between the temperature and driving-force dependence of rates supports the mechanism of electron transfer and the view that reduction in the reorganization energy can be affected by a strategically placed Lewis acid catalyst, His516H⁺. The trends that support this view hold regardless of whether electron-transfer reaction is treated as adiabatic or nonadiabatic because

mechanistic insights derive from the *change* in activation barrier as a function of pH (or mutation).

The λ estimated here may be viewed as an upper limit. The reason is the uncertainty associated with interpreting the $\log A = 8.5$ measured at low pH in terms of an adiabatic reaction. This pre-exponential term is not uncommonly small but is significantly smaller than that at high pH where $\log A = 10$. The result at low pH may indicate a larger entropic contribution to the free-energy barrier or a weaker electronic coupling, perhaps because of a greater electron-transfer distance. Analysis of the driving-force dependence of the rates using a nonadiabatic formalism and the pre-exponential factor determined in the temperature studies indicates $\Delta G^\ddagger = 3.7$ kcal mol⁻¹ at $\Delta G^{\circ'} = 0$ kcal mol⁻¹. From this value, $\lambda = 15$ kcal mol⁻¹ is determined, in good agreement with $\lambda = 14$ kcal mol⁻¹ derived from treatment of the temperature data within the nonadiabatic formalism where $E_{\text{act}} = 2.9 \pm 1.7$ is equated to ΔG^\ddagger at $\Delta G^{\circ'} = -1.3$ kcal mol⁻¹.

We note that interpretation of the experimental data may also be complicated in the case of very strong electronic coupling, when mixing of the donor and acceptor electronic wave functions causes an avoided crossing well below the intersection point of the free energy surfaces.⁴¹ This effect may explain the anomalies encountered when the Marcus cross relation is applied to electron-transfer reactions between transition metal complexes and O₂.^{7b,g} In the limit of strong electronic coupling, ΔG^\ddagger estimated from the rate constant is significantly lower than the intersection point from which λ is defined theoretically. The experimental λ , in this instance, is reduced from the theoretical value by approximately 4 times the electronic coupling energy.³⁴ We address the issue of electronic coupling herein because the assumption of the adiabatic behavior may have repercussions for the model used to understand the origin of the oxygen-18 kinetic isotope effects.

Theoretical Basis for Kinetic Isotope Effects. Within the framework of electron transfer theory, kinetic isotope effects originate from the reorganization of heavy nuclei upon converting the reactant to the product state. Reorganization of the inner-sphere modes may be formulated semiclassically, in terms of the force constant change between the reactant state and product states, or quantum mechanically, in terms of Franck–Condon (nuclear overlap) factors.⁴² The former approach is analogous to the effect of zero-point energy on the activation barrier between the reactant and transition state in semiclassical transition-state theory. The latter approach de-emphasizes thermal activation and considers instead the overlap of vibrational wave functions associated with the high-frequency bonds. In the present case, FADH⁻ reduces O₂ by outer-sphere electron transfer; that is, electron transfer occurs without concomitant bond formation to O₂⁻. The problem of calculating the oxygen-18 kinetic isotope effect is therefore simplified because only the O–O vibration needs to be considered.

A. Semiclassical Approach. The basic Marcus formalism does not account for the large heavy atom kinetic isotope effects on electron-transfer reactions. A simplifying assumption made when applying eq 3 is that reactant and product states are characterized by harmonic oscillators of the same curvature

(37) Nonadiabatic treatment of rates as a function of temperature typically neglects the entropic contributions and can result in significantly smaller estimates of λ .

(38) (a) Ortiz-Maldonado, M.; Ballou, D. P.; Massey, V. *Biochemistry* **2001**, *40*, 1091–1101. (b) Eckstein, J. W.; Hastings, J. W.; Ghisla, S. *Biochemistry* **1993**, *32*, 404–411.

(39) Miller, J. R.; Edmondson, D. E. *J. Biol. Chem.* **1999**, *274*, 23515–23525.

(40) Yorita, K.; Misaki, H.; Palfey, B. A.; Massey, V. *Proc. Natl. Acad. Sci. U.S.A.* **2000**, *97*, 2480–2485.

(41) Schutz, C. N.; Warshel, A. *J. Phys. Chem. B* **2004**, *108*, 2066–2075 and references therein.

(42) German, E. D.; Kuznetsov, A. M.; Efremenko, I.; Sheintuch, M. *J. Phys. Chem. A* **1999**, *103*, 10699–10707.

Table 4. Parameters Used To Calculate Oxygen Kinetic Isotope Effects According to Eqs 8–11

	$\hbar\omega^a$ (cm ⁻¹)	$(\Delta d)^2 \times 10^{4b}$ (cm) when $\Delta r = 0.10 \text{ \AA}$	$(\Delta d)^2 \times 10^{4b}$ (cm) when $\Delta r = 0.12 \text{ \AA}$
^{16,16} O ₂	1556.3	3.7749	5.4359
^{16,16} O ₂ ⁻	1064.8		
^{16,18} O ₂	1512.5	3.9970	5.7556
^{16,18} O ₂ ⁻	1034.8		

^a From stretching frequencies in ref 44. ^b Reduced displacement.

calculated from the classical λ_{in} and λ_{out} . This treatment minimizes the isotopic differences in ΔG^\ddagger due to the changes in force constant. The λ_{in} (eq 5) for the isotopologues of O₂ differ by only 2.7 cal mol⁻¹ which translates into a negligible 0.68 cal mol⁻¹ difference in the activation barriers.

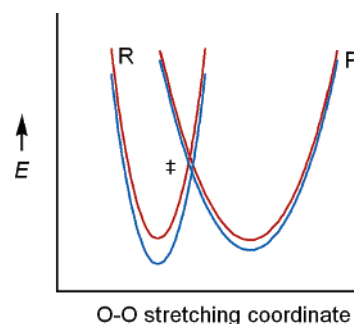
Considering the reaction of O₂ with FADH⁻, a significant isotope effect is expected because of the large change in force constant that occurs upon formation of O₂⁻. The equilibrium isotope effect on conversion of O₂ to O₂⁻ is predicted here using the Bigeleisen equation⁴³ and the vibrational energies listed in Table 4.⁴⁴ The result can be formalized in terms of Marcus theory through the effect of the isotopic ΔG° on ΔG^\ddagger . This approach considers the influence of the equilibrium isotope effect on the kinetic isotope effect by a vertical offsetting of the reactant and product harmonic oscillators.

Because the isotope effect on the reduction potential of O₂ is impossible to determine with conventional electrochemical techniques, $\Delta G^\circ_{18} - \Delta G^\circ_{16}$ must be calculated from the equilibrium isotope effect for the half-reaction where O₂ is converted to O₂⁻. The ¹⁸K = 1.0331 previously calculated⁴⁴ corresponds to $\Delta G^\circ_{18} - \Delta G^\circ_{16} = 19.3 \text{ cal mol}^{-1}$. This difference may be taken into consideration through eq 7, which was derived from eqs 3 and 6 by neglecting isotopic differences in λ and the pre-exponential terms. A similar equation has been used to estimate solvent isotope effects on electron transfer.^{45,46}

$$\ln\left(\frac{k_{16}}{k_{18}}\right) = \left(\frac{\Delta G^\circ_{18} - \Delta G^\circ_{16}}{2RT}\right) \left(1 + \frac{\Delta G^\circ_{18} + \Delta G^\circ_{16}}{2\lambda}\right) \quad (7)$$

Equation 7 is accurate in the normal driving-force regime where it predicts a linear increase in the kinetic isotope effect as ΔG° becomes more positive. Assuming $\Delta G^\circ_{16} = 0 \text{ kcal mol}^{-1}$ and $\Delta G^\circ_{18} - \Delta G^\circ_{16}$ estimated above, the kinetic isotope effect ¹⁸k (defined as k_{16}/k_{18}) = 1.0164. For the most unfavorable reaction of glucose oxidase examined, where $\Delta G^\circ_{16} = 2.0 \text{ kcal mol}^{-1}$ and $\lambda = 28 \text{ kcal mol}^{-1}$, an increase in ¹⁸k to 1.0176 is predicted. Lower reorganization energies translate into a greater sensitivity of the isotope effect to changes in reaction driving force. For example, ¹⁸k = 1.0186 is calculated for $\Delta G^\circ_{16} = 2.0 \text{ kcal mol}^{-1}$ and $\lambda = 15 \text{ kcal mol}^{-1}$. Clearly, neither the magnitude nor the trend in ¹⁸k_{cat}/K_M with ΔG° is reproduced by this simple model.

A slightly more complex model is required to explicitly treat the change in force constant that occurs on converting the

**Figure 6.** Representation of the semiclassical oxygen-18 isotope effect on the reduction of O₂ to O₂⁻.

reactant to the product. A simple analytical expression for the dependence of the isotope effect on reaction driving force for harmonic oscillators with unequal curvatures is described in the Appendix section. The key elements of this treatment are the use of force constants for O₂ and O₂⁻ and the experimental bond length difference ($\Delta r = 0.12 \text{ \AA}$).⁴⁷ The ΔG°_{16} between reactant and product is varied while keeping $\Delta G^\circ_{18} - \Delta G^\circ_{16}$ constant. The case where $\Delta G^\circ_{16} = 0 \text{ kcal mol}^{-1}$ is shown graphically in Figure 6 and a plot of calculated isotope effect versus driving-force given in the Appendix. The calculated ¹⁸k = 1.0195 at $\Delta G^\circ_{16} = 0$ is only slightly larger than that predicted by eq 6 for the case where the λ and the curvatures of the free-energy surfaces are assumed to be equal. This analysis illustrates that the isotope effects upon electron transfer to O₂ cannot be described using traditional approaches which consider only differences in activation barriers due to changes in force constants and free energies.

B. Quantum Mechanical Approach. In quantum mechanical electron-transfer theory, vibrational modes with frequencies that are high relative to the thermal energy are treated as frozen. Therefore, the contribution of the high-frequency modes does not appear in the classical λ_{in} but in the pre-exponential part of eq 6. Because the frequency of the O–O stretch in O₂ is 1556.3 cm⁻¹ and significantly higher than the available thermal energy ($k_B T \approx 207 \text{ cm}^{-1}$ where k_B is Boltzmann's constant and $T = 25 \text{ }^\circ\text{C}$), this mode is properly treated in the quantum mechanical limit. In this description, nuclear displacement occurs by tunneling rather than by thermal activation of the O–O bond.

Jortner and co-workers have advanced the use of the quantum mechanical formalism given by eq 8 to describe electronically nonadiabatic electron-transfer reactions as a function of an electronic coupling term (H_{12}) and a thermally averaged Franck–Condon factor (G).⁴⁸ The latter includes contributions from the electronic energy gap (ΔE), the thermally averaged solvent modes (E_s), and the quantized intramolecular vibrations (ω' and ω'' , corresponding to the reactant state and product state, respectively). The first and second terms are the temperature-independent analogues of ΔG° and λ in eq 3. The tunneling probability associated with high-frequency modes is defined in terms of a reduced displacement factor (Δd)² for the n modes that distort upon vibration. The reduced displacement parameter, given by eq 9 in units of cm, includes the difference in

(43) Huskey, P. W. In *Enzyme Mechanism for Isotope Effects*; Cook, P. F., Ed. CRC Press: Boca Raton, FL, 1991.

(44) Tian, G.; Klinman, J. P. *J. Am. Chem. Soc.* **1993**, *115*, 8891–8897.

(45) Guarr, T.; Buhks, E.; McLendon, G. *J. Am. Chem. Soc.* **1983**, *105*, 3763–3767.

(46) Weaver, M. J.; Nettles, S. M. *Inorg. Chem.* **1980**, *19*, 1641–1646.

(47) Vaska, L. *Acc. Chem. Res.* **1976**, *9*, 175–183.

(48) (a) Buhks, E.; Bixon, M.; Jortner, J.; Navon, G. *J. Phys. Chem.* **1981**, *85*, 3759–3762. (b) Buhks, E.; Bixon, M.; Jortner, J. *J. Phys. Chem.* **1981**, *85*, 3763–3766.

Table 5. Calculated Y Factors and Oxygen-18 Kinetic Isotope Effects for the Reduction of O_2 to O_2^- When $\Delta G^{\circ'} = 0^a$

temp (°C)	^{16}Y (0.10 Å)	^{18}Y (0.10 Å)	$^{18}k_{qm}$ (0.10 Å)	^{16}Y (0.12 Å)	^{18}Y (0.12 Å)	$^{18}k_{qm}$ (0.12 Å)
10	2.7238	2.7798	1.0288	3.9224	4.0028	1.0418
25	2.6824	2.7350	1.0270	3.8628	3.9384	1.0393
40	2.6397	2.6893	1.0254	3.8013	3.8726	1.0370

^a Δr values given in parentheses.

equilibrium bond lengths in the reactant and the product states (Δr) and the reduced mass (m); \hbar is Plank's constant divided by 2π .

$$W = (2\pi/\hbar)|H_{12}|^2 G(\Delta E, E_s, \{\Delta d\}, \{\omega'\}, \{\omega''\}, T) \quad (8)$$

$$(\Delta d)^2 = \frac{n(\Delta r)^2 m}{\hbar} \quad (9)$$

According to the equations above, the intramolecular reorganization energy can be divided into terms corresponding to frequency changes and nuclear displacements. As demonstrated for the classical model, a relatively small contribution to the kinetic isotope effect arises from frequency changes alone. In the quantum model, the dominant isotope effect results from the differences in the Franck–Condon overlap factors. These factors describe the probability of nuclear positions at the instant of electron transfer and are related to the exponential Y terms defined in eq 10. The equation for Y was derived for an electron self-exchange reaction and contains contributions from $(\Delta d)^2$ and the ω characterizing the reactant and product states. By definition, eq 11 gives the kinetic isotope effect in terms of the influence of symmetric vibrational modes on Y .⁴⁸

$$Y = 2(\Delta d)^2 \omega' \omega'' [\omega' \coth \nu'' + \omega'' \coth \nu']^{-1} \quad (10)$$

$$\text{where } \nu' = \frac{\hbar \omega'}{4k_B T} \text{ and } \nu'' = \frac{\hbar \omega''}{4k_B T}$$

$$\ln\left(\frac{k_{16}}{k_{18}}\right) = Y_{18} - Y_{16} \quad (11)$$

The kinetic isotope effects on reduction of O_2 is estimated as one-half the isotope effect on the self-exchange reaction between O_2 and O_2^- (eq 11), following an approach which has been previously described.^{45,48} The calculated isotope effects designated $^{18}k_{qm}$ are presented in Table 5 for the case where $\Delta G^{\circ'} = 0$. The Franck–Condon factors and, consequently, the calculated isotope effects are very sensitive to bond distances and moderately sensitive to temperature. The results of the calculations as a function of these parameters are presented in the table. For $\Delta r = 0.1$ Å the calculated $^{18}k_{qm} = 1.027$ in excellent agreement with the experimentally observed values. The $^{18}k_{qm}$ increases to 1.039 for $\Delta r = 0.12$ Å, which is closer to the experimentally determined difference in bond lengths for O_2 and O_2^- .^{7b,42,45}

A unique feature of this quantum mechanical model is that the isotope effect comes from intrinsic factors requiring no contribution from $\Delta G^{\circ}_{18} - \Delta G^{\circ}_{16}$ to reproduce the magnitude of the experimental values. However, the isotope effect is expected to be dependent on the reaction driving force due to changes in the Franck–Condon overlap factors. In contrast, the semiclassical model de-emphasizes the influence of the intrinsic reorganization energy and predicts a kinetic isotope effect that

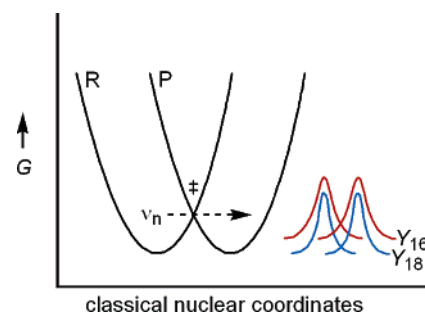


Figure 7. Representation of the quantum mechanical oxygen-18 isotope effect on the reduction of O_2 to O_2^- .

is almost completely thermodynamic in origin. The neglect of intrinsic quantum mechanical contributions from high frequency stretching modes is likely the reason that this model underestimates the experimentally observed values. Furthermore, the quantum model predicts that the kinetic isotope effect may exceed the calculated equilibrium isotope effect. In previous semiclassical treatments of isotope effects on reactions of O_2 , this possibility had not been recognized.^{8a}

The origin of the kinetic isotope effect is depicted in Figure 7 in terms of the Franck–Condon overlap factors. Reorganization of the thermally averaged low-frequency modes of the surroundings gives rise to the reaction barrier, and nuclear tunneling occurs from an activated nuclear configuration at the intersection of the reactant and product states. Extension of this model to the present work suggests that the oxygen nuclei tunnel through the barrier imposed by reorganization of the surrounding protein. The agreement between the predictions of the quantum mechanical model and the observed kinetic isotope effects is perhaps fortuitous because the application of the formalism to electronically adiabatic electron transfers is not rigorously correct. Alternative formalisms which treat nuclear tunneling as a correction to the classical rate expression are available.⁴⁹ Along these same lines, Hammes–Schiffer and co-workers have derived a rate expression in which the overall nonadiabatic nature of the reaction is determined by the coupling between mixed electronic and vibrational (vibronic) states, allowing the possibility of overall nonadiabatic behavior for reactions that are electronically adiabatic.^{50,51}

C. Comparison to Previous Studies. McLendon and co-workers reported the first study of heavy atom kinetic isotope effects on electron-transfer reactions as a function of reaction driving force.⁴⁵ Noncompetitive kinetic isotope effects on the oxidation of $[Fe^{II}(H_2O)_6]^{2+}$ to $[Fe^{III}(H_2O)_6]^{3+}$ were determined and found to vary from $^{18}k = 1.09(2)$ to $1.04(1)$ as ΔG° varied from -8.1 kcal mol⁻¹ to -17 kcal mol⁻¹ and decreased to unity for $\Delta G^{\circ} = -35$ kcal mol⁻¹. The isotope effects were explained by tunneling of the Fe–O breathing modes with frequencies that ranged from 390 to 490 cm⁻¹. Prior to this work, the importance of nuclear tunneling had been discussed at length in the context of electron transfer at very low temperatures in photosystem II.⁵² The subject has been revisited in a more recent review.⁵³ While the inability of the semiclassical Marcus theory to reproduce the heavy atom kinetic isotope effects on electron-

(49) Brunschwig, B. S.; Logan, J.; Newton, M. D.; Sutin, N. *J. Am. Chem. Soc.* **1980**, *102*, 5798–5809.

(50) Soudackov, A.; Hammes-Schiffer, S. *J. Chem. Phys.* **2000**, *113*, 2385–2396. See ref 51 for a related discussion.

(51) Creutz, C.; Sutin, N. *J. Am. Chem. Soc.* **1988**, *110*, 2418–2427.

(52) Devault, D. *Quart. Rev. Biophys.* **1980**, *13*, 387–564.

transfer reactions provides support for the quantum mechanical view, the applicability of the model to cases where there is strong electronic coupling characterizing the transition from reactant to the product state remains unclear.

This is only the second study of the oxygen-18 kinetic isotope effect as a function of reaction driving force. Here the isotope effects are measured competitively and with very high precision. Analysis of error-weighted data suggests that the isotope effect is independent of driving force within the error limits, varying only slightly from 1.0279(6) to 1.0266(5) as the reaction free energy varies from -1.3 to $+2.0$ kcal mol⁻¹. This observation is difficult to reconcile with a semiclassical model which predicts that the isotope effects should increase from 1.0162 to 1.024 over the same range (see Appendix Figure 8). In agreement with the findings from studies of isotope effects on electron-transfer reactions of transition metal complexes,^{45,48} the quantum mechanical formalism yields theoretical values which are consistent with the observed effects on reactions of O₂ (see Table 5).

Jortner and co-workers^{48a} have used a saddle-point approximation to model the response of Franck–Condon overlap factors to changes in reaction driving force. The parabolic function indicated a maximum isotope effect at $\Delta G^\circ = 0$ where the difference in nuclear overlap factors for the isotopologues is the greatest. The variations from the maximum are caused by increased overlap factors which arise from the population of vibrationally excited states. In the model, the breadth of this saddle point is determined by the contribution of the outer-sphere reorganization energy, the frequency of the isotope sensitive mode and the reaction temperature. When the activation energy associated with outer-sphere modes is large relative to that associated with the high-frequency inner-sphere modes, the isotope effect is insensitive to driving force.⁴⁸ Thus, as reported here, the relatively flat trend in isotope effect with modest variations from $\Delta G^\circ = 0$ is consistent with a large contribution of λ_{out} to the reaction barrier.

D. Applications to Enzymatic O₂ Activation. Heavy atom kinetic isotope effects have historically been interpreted within the framework of transition state theory,⁵⁴ yet an apparent contradiction arises when the reaction coordinate is not a bond-stretching mode. This situation obtains, for electron transfer, reactions of O₂ which are characterized by large λ_{out} . In the semiclassical transition state theory, the oxygen kinetic isotope effect would be predicted to increase and approach the equilibrium value as a reaction becomes more endothermic and the transition state more closely resembles the product O₂⁻.^{8a} The lack of trend observed in this study is, therefore, opposite to expectations based on the semiclassical view.

The present results expose the need for a unique framework to understand kinetic isotope effects on electron transfer to O₂, a reaction which takes place in a wide variety of chemical and biological processes. A quantum mechanical view of the heavy atom kinetic isotope effect is a dramatic departure from semiclassical views as illustrated by our prediction that the kinetic isotope effects may exceed the equilibrium isotope effects; however additional experimental evidence is needed to unequivocally support or refute the quantum mechanical model.

Oxygen-18 isotope effects have been measured on reactions in biological systems for processes ranging from reversible binding of O₂ to metal sites,⁴⁴ combination of O₂ and an organic radical⁵⁵ and the reduction of O₂ with concomitant bond formation to a redox metal.^{56–60} The reactions of glucose oxidase provide the only clear examples of isotope effects on outer-sphere electron transfer to O₂.¹⁴ In most cases, measured isotope effects fall within the limits set by the equilibrium values although the kinetic complexity that exists in many enzymatic processes may obscure such interpretations.

Currently, oxygen-18 kinetic isotope effects serve as rough diagnostics for changes in oxygen bonding that occur in or before the rate-determining step of enzyme reactions. In principle, a single isotope effect can be correlated with the structure of an activated O₂ intermediate and the type of reaction this species undergoes. Such application requires a predictive understanding of how isotope effects vary with mechanism as well as parameters such as reaction driving force and temperature. In the context of unanswered questions regarding the appropriate physical model for interpreting the oxygen kinetic isotope effects, studies of model systems have been initiated (by J.P.R.) to address these issues.

Experimental Section

Glucose oxidase from *Aspergillus niger* was overexpressed as a 320 kDa hyperglycosylated protein^{14,12} or obtained commercially as a ~160 kDa from Sigma-Aldrich or Boehringer Mannheim.²⁰ The H516A (320 kDa variant) was overexpressed as described previously.¹⁴ The apo-protein was prepared starting from concentrated solutions of holoprotein (100 mg/mL). Following dialysis against phosphate buffer (0.025 M, pH 6, glycerol 30% w/v), approximately 5 mL of the holoprotein solution was diluted 2-fold with acidic phosphate buffer (0.025 M, pH 1.1, glycerol 30% w/v) resulting in a solution buffered to pH 1.7 at 0 °C. This solution was protected from light and stirred at 0 °C for 30 min. The FAD liberated from the partially unfolded protein was removed by size exclusion chromatography on a Biogel p-10 column (ca. 6.5 cm × 30 cm) pre-equilibrated with the phosphate buffer (0.025 M, pH 1.1, glycerol 30% w/v) at 4 °C with a flow rate of 7 mL min⁻¹.

The colorless apo-protein eluted within 10 to 20 min in two to four 20–30 mL fractions. The fractions were collected in tubes containing 8 mL phosphate buffer (0.4 M, pH 8.0), charcoal (100 mg) and Dextran 70 (20 mg). The suspensions containing apo-protein were instantly adjusted to pH 7 ± 1. The combined fractions were stirred for 60 min protected from light prior to filtration through a medium porosity glass frit. The apo-protein was concentrated using an Amicon “stirred cell” containing a cellulose membrane with either a 30 or 50 kDa molecular weight cutoff. The apo-protein, concentrated at least 5-fold after 2 to 3 h at 4 °C, was then separated into 2 mL fractions and stored at -80 °C.

On a preparative scale holoproteins were obtained by incubation of the apo-protein at 4 °C for 24 h with 2–5 equiv of the appropriate flavin. The flavins were prepared and analyzed for purity by published protocols,¹⁷ stored at -80 °C and used without further purification.

(53) Barbara, P. F.; Meyer, T. J.; Ratner, M. A. *J. Phys. Chem.* **1996**, *100*, 13148–13168.

(54) Melander, L.; Saunders, W. H. *Reaction Rates of Isotopic Molecules*; Wiley: New York, 1980.

(55) Glickman, M. H.; Cliff, S.; Thiemens, M.; Klinman, J. P. *J. Am. Chem. Soc.* **1997**, *119*, 11357–11361.

(56) (a) Mills, S. A.; Goto, Y.; Su, Q.; Plastino, J.; Klinman, J. P. *Biochemistry* **2002**, *41*, 10577–10584. (b) Su, Q.; Klinman, J. P. *Biochemistry* **1998**, *37*, 12513–12525.

(57) (a) Tian, G.; Berry, J. A.; Klinman, J. P. *Biochemistry* **1994**, *33*, 226–234. (b) Francisco, W. A.; Blackburn, N. J.; Klinman, J. P. *Biochemistry* **2003**, *42*, 1813–1819.

(58) Francisco, W. A.; Tian, G.; Fitzpatrick, P. F.; Klinman, J. P. *J. Am. Chem. Soc.* **1998**, *120*, 4057–4062.

(59) Stahl, S. S.; Francisco, W. A.; Merx, M.; Klinman, J. P.; Lippard, S. J. *J. Biol. Chem.* **2001**, *276*, 4549–4553.

(60) Burger, R. M.; Tian, G.; Drlica, K. *J. Am. Chem. Soc.* **1995**, *117*, 1167–1168.

Following enzyme reconstitution, excess flavin was removed by centrifugation using a Micro-con Ultra-free filter with 30 kDa molecular weight cutoff at 4 °C. Repeated washings with phosphate buffer (0.025 M, pH 6.0) were necessary to remove the excess flavin. The concentration of active enzyme was determined by titration with glucose or 2-deoxyglucose under oxygen-free conditions using a Hewlett-Packard 8452A spectrophotometer. The bleaching of the absorbance at ca. 450 nm indicated the disappearance of bound FAD and the formation of FADH⁻. The titration measurements indicated that the commercial enzyme and the recombinant 320 kDa enzyme prepared by overexpression of glucose oxidase behaved identically, each apo-enzyme incorporating 2 equiv of flavin per homodimer. Most enzyme preparations used in kinetic studies exhibited 100% activity. For preparations with less than 100% activity, a correction for the titratable concentration of flavin was applied. The corrected rate constants for enzymes exhibiting 20–50% of the expected activity were in excellent agreement with rate constants determined using the holoproteins deemed to be 100% active.

Rate measurements were performed using a biological oxygen analyzer (Yellow Springs Inc.) which consisted of an O₂ sensor (Clark electrode) and a voltmeter. Temperature was controlled ± 0.01 °C using a Neslab circulating bath. Substrate solutions contained either 1-¹H-2-deoxyglucose (Sigma, Grade III) or 1-²H-2-deoxyglucose (Cambridge Isotope Laboratories) of at least 98% purity. Ionic strength was maintained at $\mu = 0.1$ M using sodium acetate (0.164 M) at pH 5.0, sodium pyrophosphate (0.012 M) at 9.0, and sodium hydroxide/2-deoxyglucose (0.1 M) at pH 12.5. Solutions used to measure k_{cat}/K_M (sugar) were allowed to stand for 24 h at room temperature prior to use to ensure that equilibration of the anomeric sugars was complete. Reactions were initiated by addition of 1–10 μL of enzyme solutions of varying concentrations. The reported kinetic data and isotope effects were determined to be reproducible from batch to batch of both enzyme and substrate.

Oxygen kinetic isotope effects were measured using a custom designed apparatus that has been previously described.^{57a} Solutions contained ¹H-2-deoxyglucose (3 to 6 $\times 10^{-2}$ M) and high concentrations of O₂ (0.5 to 1.0 $\times 10^{-3}$ M). Each isotope effect was determined from at least six measurements, four of which were made on different solutions. Samples of unreacted O₂ from 20% to 100% of the initial concentration were converted to CO₂ and flame-sealed in glass tubes. The samples were analyzed by isotope ratio mass spectrometry at Geochron (Krueger) Laboratories in Cambridge, MA.

Kaleidagraph (Synergy Software) was used for kinetic analysis. All parameters are reported to two standard errors. Nonlinear regression was performed when fitting data to the Michaelis–Menten expression and eq 2. Weighting was applied in some cases, and the results of the unweighted data provided for comparison.

Conclusions

We have used chemically modified flavin cofactors to perform a systematic analysis of the oxidative half-reaction that occurs during catalysis by glucose oxidase. When bound to glucose oxidase, the modified flavins reduce O₂ with net electrochemical potentials that vary from 0.055 V to –0.085 V. Over this range, rates and oxygen-18 kinetic isotope effects have been examined. Several new insights emerge from these studies.

Kinetic analysis reveals a linear free-energy relationship between rates of O₂ reduction and the driving force for outer-sphere electron transfer. Rate constants vary by a factor of almost 20 over the ~ 3 kcal mol⁻¹ range in ΔG° , which is comparable to the size of the activation barrier. The data expose an irreversible electron-transfer step during the oxidative half-reaction and agree well with previous studies of rates as a function of temperature. Using driving-force and temperature

studies together, electron transfer in the active site of glucose oxidase has been analyzed and the reorganization energy refined to $\lambda = 28 \pm 7$ kcal mol⁻¹ using an adiabatic model.

The aggregate data support an earlier proposal¹⁴ that glucose oxidase catalyzes electron transfer to O₂ at low pH by lowering of the reorganization energy by at least 12 kcal mol⁻¹ relative to the uncatalyzed reactions in aqueous solution,^{7b} in the wild-type enzyme at high pH, and in the H516A mutant at low pH. The active site His516 is therefore implicated in rate acceleration of more than 3 orders of magnitude. The results highlight the importance of pH-dependent electrostatic effects during electron transfer in proteins and illustrate how preorganization of an active site can serve as an origin for enzyme catalysis.⁶¹

Despite having a $\Delta G^{o'}$ that is close to zero, the reaction of glucose oxidase with O₂ occurs with a low activation barrier at the pH optimum. The observation of nearly indistinguishable oxygen-18 kinetic isotope effects on reactions of enzyme-bound flavins indicates that the barrier is dominated by reorganization of the solvated protein. The present results may be generalized and extended to other enzymes, in particular ones that form O₂⁻ during a critical step in the O₂ activation process. On the basis of the agreement between experiment and theory, we propose that $^{18}k \approx 1.027$ will be characteristic for a variety of reactions that occur by outer-sphere electron transfer. The benchmark value is predicted to be quite robust because of the expected dominant contribution from outer-sphere reorganization energy for this class of reactions.

Acknowledgment. This work was supported by grants from the NIH to J.P.K. (GM 25765) and J.P.R. (GM 20709). J.P.R. is grateful to Sharon Hammes Schiffer (Penn State University) and David Yarkony (Johns Hopkins University) for helpful discussions.

Appendix

The method used to calculate isotope effects by solving for differences in the energy barrier defined by the intersection points of harmonic oscillators with unequal curvatures is described. Two equations are required corresponding to O₂ (eq A1) and O₂⁻ (eq A2) within the harmonic oscillator approximation.

$$y_1 = \frac{1}{2}k_1x^2 \quad (\text{A1})$$

$$y_2 = \frac{1}{2}k_2(x - x_0)^2 - \Delta G^\circ \quad (\text{A2})$$

The force constants are derived from the stretching frequencies (Table 4) within the Born–Oppenheimer approximation.⁶² The O–O stretch is characterized by $k_1 = 1143.27$ kcal mol⁻¹ Å⁻² in O₂ and $k_2 = 535.142$ kcal mol⁻¹ Å⁻² in O₂⁻. The variable x reflects displacement from the equilibrium nuclear position. The x_0 is a constant set at 0.12 Å for the difference in bond lengths for O₂ and O₂⁻. The parameter ΔG° is the overall reaction driving force corrected by the difference in isotopic zero-point energy levels in O₂ and O₂⁻ (19.3 cal mol⁻¹).

(61) (a) Warshel, A. *J. Biol. Chem.* **1998**, 273, 27035–27038. (b) Muegge, I.; Qi, P. X.; Wand, A. J.; Chu, Z. T.; Warshel, A. *J. Phys. Chem. B* **1997**, 101, 825–836.

(62) Jensen, J. O.; Yarkony, D. R. *J. Chem. Phys.* **1988**, 89, 975–983.

To solve for the intersection point, the two equations are set equal and recast in the general expression

$$(A_1 - A_2)x^2 + (B_1 - B_2)x + (C_1 - C_2) = 0 \quad (\text{A3})$$

to obtain

$$\left(\frac{1}{2}k_1 - \frac{1}{2}k_2\right)x^2 + (k_2x_0)x + \left(\Delta G^\circ - \frac{1}{2}k_2x_0\right) = 0 \quad (\text{A4})$$

The quadratic expression

$$x = \frac{-k_2x_0 \pm \sqrt{(k_2x_0)^2 - 2(k_1 - k_2)\left(\Delta G^\circ - \frac{1}{2}k_2x_0\right)}}{(k_1 - k_2)} \quad (\text{A5})$$

is solved for x . The root of x corresponding to the distance at the intersection point which lies between the minima of the harmonic functions is substituted into eq A1 to calculate y , the ΔG^\ddagger . The isotopic difference in ΔG^\ddagger is related to the kinetic isotope effect ^{18}k (written as the ratio k_{16}/k_{18}) through the expression

$$\frac{k_{16}}{k_{18}} = \exp\left(\frac{\Delta G^\ddagger_{18} - \Delta G^\ddagger_{16}}{RT}\right) \quad (\text{A6})$$

A plot of calculated and experimental ^{18}k versus reaction driving force is shown in Figure 8. When harmonic oscillators

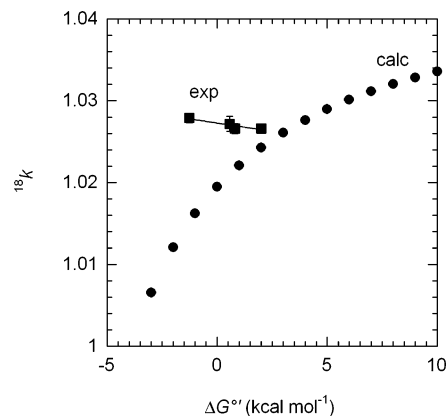


Figure 8.

have equal curvature, the treatment reproduces the isotope effect calculated using eq A7, which is the same as eq 7 described in the text.

$$\frac{k_{16}}{k_{18}} = \exp\left(\frac{\Delta G^\circ_{18} - \Delta G^\circ_{16}}{2RT}\right) \left(1 + \frac{\Delta G^\circ_{18} + \Delta G^\circ_{16}}{2\lambda}\right) \quad (\text{A7})$$

Supporting Information Available: A plot of rates as a function of temperature for glucose oxidase and the H516A variant. This material is available free of charge via the Internet at <http://pubs.acs.org>.

JA047050E